JOURNAL OF SOLID STATE CHEMISTRY 46, 1–22 (1983)

Quantitative Correlations of Deviations from Ideality in Binary and PseudoBinary Solid Solutions

P. K. DAVIES AND A. NAVROTSKY

Department of Chemistry, Arizona State University, Tempe, Arizona 85287

Received April 29, 1982; in final form July 16, 1982

Deviations from ideal mixing in a number of isostructural binary solid solutions are parameterized using regular and subregular thermodynamic mixing models. Linear correlations between calculated interaction parameters and a term representing the volume mismatch of the two end-members are obtained. These correlations apply to a wide variety of structure types and are found to segregate the solid solutions according to the valence of the ions being mixed. Alkali halide systems show smaller relative deviations than oxide and chalcogenide systems. The ratio of the slopes of these correlations agree with predictions made from consideration of the effective charges of the ions being mixed. The correlations are used to predict the variation of critical temperature, and composition, as a function of component volume mismatch. Calculations of the free energies of transformation of rock salt to nickel arsenide structures and of wurtzite/sphalerite (fourfold coordination) to rock salt/nickel arsenide (sixfold coordination) structures are made using the interaction parameters predicted by the correlations and observed terminal solid solubility data.

Introduction

Thermodynamic modeling of solid solution formation is of interest both from a practical and theoretical point of view. The mixing properties influence solid solubilities, physical properties, diffusion coefficients, and the distribution of components among coexisting solid and liquid phases. Calculation of phase boundaries at temperatures and pressures other than those at which the original phase relations were determined is made possible if the energetics of the formation of the solid solution are known. This leads to one important geochemical application, namely, that of mineral geothermometry and geobarometry. Solid solution formation is also an important phenomenon in the evaluation of high-temperature equilibria encountered in the production and refining of metals and alloys; indeed most present theories of solid solution formation originate from work done on alloy systems (*1*).

Theoretical modeling of solid solution formation is useful since one is able to gain insight into the factors, on an atomic scale, governing the energetics of the solid solution. A solid solution of given composition will only be stable if its free energy is less than that of an equivalent mechanical mixture of its components, or of any possible exsolution products. Several factors directly affect the thermodynamics of solid solutions and consequently the limits of solid solubility. The first major criterion for solid solubility is structural type. Generally, complete miscibility between noniso-

0022-4596/83/010001-22$03.00/0

structural end-members is not possible. Special cases can arise where complete miscibility may occur. For example, ilmenite and corundum, for which one space group ($R\bar{3}$) is a subgroup ($R\bar{3}c$) of the other, could show complete solubility (*2*) or only second-order transitions. However, usually only mutual terminal solubility occurs in nonisostructural systems (*3*).

In isostructural systems four main factors can affect the range and stability of solid solution. The first and usually most important is the size difference of the ions or atoms being mixed. This results in a strain energy which is larger the greater the difference in size. For a given size difference, it is often easier to put a smaller atom into a larger host lattice than vice versa. This effect is illustrated by asymmetric solubility relations in binary systems. Solubility of the smaller ion in the structure with larger volume is more extensive than solubility of the larger ion in the smaller structure. The effect of size difference upon solid solution thermodynamics has formed the basis of most theoretical models of binary solid solutions (*4–6*). The second factor affecting solid solution formation is that of differences in bonding character. In cases where the covalency (ionicity) of the ions being mixed differs significantly, one would expect solubility to be limited, even when the ions are similar in size. Examples are NaCl–AgCl and NaBr–AgBr, which show large positive deviations in their heats of mixing (*7*). Valence of the ions being mixed can also affect the limits of solubility, ions of higher valence mixing less favorably than ions of lower valence, for a given size difference.

When solid solution involves transition metal ions, electron configuration effects can play a significant role in determining the stability of the solution.

Some efforts have been made to systematize solid solution behavior in binary systems; these range from purely theoretical approaches (*4, 5*) to semiempirical treatments (*6, 8*).

The theoretical models have largely been limited to alloy and alkali halide systems (*1, 4*) and have met with considerable success. A rigorous calculation of the partition function for ionic crystals, when the nearest neighbors of the cations (namely, the anions) remain the same, but the next-nearest neighbors change, immediately gives rise to difficulties in the definition of a pair interaction energy. This approach, which was successful for alloys, is therefore difficult for ionic crystals. In such cases most theoretical models calculate a form of strain energy, or allow for local relaxation about a given ion.

Fancher and Barsch (*4, 9, 10*) modeled eight alkali halide systems using the classical Born theory of ionic crystals to calculate the formation energy of point defects (*11*). The quality of this treatment is dependent upon the form of the interatomic potential used and on approximations made in calculating atomic displacements around the defect. Input parameters were lattice constants, compressibilities, and electronic polarizability data. The calculated heats of formation agreed well with experimental data. The initial calculation assumed a random distribution of substituted ions and therefore an ideal configurational ΔS_{mix}. As in metallic alloys, vibrational excess entropies were found to play an important role in these halides. The excess vibrational contributions may be calculated directly from the dependence of heat capacity on composition, or from the Debye temperatures of the solid solutions. Calculations were made using elastic constants and bulk moduli (*4*). The excess vibrational entropy contributions in the alkali halide systems were found to be as high as 20% of the configurational term.

Papers by Urusov (*5, 12*) have also used a "Born-type" approach, but ionicity differences were taken into account. Urusov

proposed that the mixing enthalpy of a given system is a result of differences in size and effective charge of the substituents and a consequence of deformation of the crystal structure and the changing of chemical interactions.

For cases in which the electronegativity difference is small, Urusov related ΔH_{mix} to a bond-length mismatch parameter (*12*). He related bond-length mismatch to volume mismatch for cubic crystals and obtained the expression

$$\Delta H_{mix} = cX_1X_2nz^2\delta^2, \qquad (1)$$

with c an empirical parameter, n the coordination number, z the charge, and

$$\delta = \left(\frac{\sqrt[3]{V_2} - \sqrt[3]{V_1}}{X_1\sqrt[3]{V_1} + X_2\sqrt[3]{V_2}}\right), \qquad (2)$$

1 and 2 being the two components.

This expression emphasizes that miscibility limits and deviations from ideality are determined by difference in total volume rather than differences in the size of the ions being mixed. Comparison of Ba–Ca mixing in various systems illustrates this point. In BaO–CaO solubility is limited (*13*), whereas for Ba_2SiO_4–Ca_2SiO_4, where the volume difference is a smaller percentage of the total volume, complete miscibility is found (*14*).

Semiempirical treatments of solid solution formation in oxide systems with rock salt structure have been discussed by Driessens (*15*) and Navrotsky (*6*). Driessens modeled data for some oxide systems using a regular solution approach. In oxide systems having the rock salt structure, experimental activity data shows that all systems, with the exception of NiO–MgO (*16, 17*), are either ideal or deviate positively from ideality. Driessens found a regular solution model to be a good approximation for all the rock salt oxides, though later work by Catlow *et al.* (*18*) has shown this is not necessarily the case, a subregular model being required to describe the NiO–MnO system. Driessens attempted to calculate the contribution to the interaction parameter from cation pair interactions by subtracting, from the experimental parameter, calculated contributions from lattice energy and crystal field stabilization. The lattice energy contribution is a result of the difference in size of the ions being mixed, which results in a change in the Coulomb attractive and Born repulsive forces in the crystal. Again these were calculated using a model based on the Born approximation. The contribution of this crystal energy to the heat of mixing is always found to be positive. The crystal field stabilization contributions for transition metal systems was calculated from numerical values of the stabilization energy given by Dunitz and Orgel (*19*). It was assumed that the stabilization energy is inversely proportional to the metal–oxygen distance.

Navrotsky (*6*) also used a regular solution approach in the modeling of deviations from ideality in some rock salt oxide systems. An approximately linear dependence was found for W, the interaction parameter, on δ^2, the square of a normalized size difference parameter, with, for component oxides 1 and 2, a_0 the lattice parameter:

$$\delta = \frac{a_{0,1} - a_{0,2}}{a_{0,1} + a_{0,2}}. \qquad (3)$$

A similar size difference parameter was used by Kleppa (*20*) in the modeling of deviations from ideality in fused salt systems. A linear correlation was obtained between δ^2 and, in the molten salt case, negative deviations from ideality. This negative deviation is a result of the decrease in next-nearest-neighbor repulsive interactions as the size difference of the ions being mixed increases. Without long-range order, strain energy terms resulting from lattice constraints play no role in fused salt systems (*21*).

The present work also uses a semiempirical approach to the problem of parameterization of binary solid solution thermodynamics. Using regular and subregular (Margules) thermodynamic models, deviations from Raoultian behavior are parameterized in terms of a volume mismatch term in binary solid solutions where no cation redistribution over inequivalent sites occurs.

Thermodynamic Formalisms

In this section the thermodynamic models used and their application to available experimental data are described.

Three main experimental methods are used in the study of the thermodynamics of binary solid solution formation. The first technique is that of solution calorimetry which allows direct determination of enthalpies of mixing (*22*). However, few such studies have been conducted and thus such results are generally not available. The second technique involves measurement of activity–composition relations, which enables calculation of excess free energies of mixing. Activity–composition relations are seldom accurate enough to warrant fitting to equations with several free parameters; however, such measurements do allow reliable modeling using regular and subregular thermodynamic approaches. Many determinations have been made on oxide systems using either gas equilibration or solid-state galvanic cell techniques.

The third method of study of solid solution formtion is determination of solubility relations. In this method compositions are analyzed by X-ray, microscopic, and/or microprobe techniques after equilibration at known temperatures and pressures. In this way the subsolidus phase diagram for the system may be constructed. Many solubility relations have been determined in this way and results obtained in some sulfide (*23*), oxide (*24*), alkali halide (*25*), tungstate (*26*), and molybdate (*27*) systems will be referred to later.

It is possible to relate regular and subregular thermodynamic models to the available experimental data. In the subregular model the free energy of mixing of a binary solid solution involving ionic mixing on 1 mole of equivalent sites is represented by

$$\Delta G_{\text{mix}} = X_1X_2]AX_2 + BX_1] + RT[X_1 1nX_1 + X_2 1nX_2], \quad (4)$$

where the component with smaller molar volume is labeled 1, the larger component 2. A is the Margules parameter for the smaller component and B is the parameter for the larger component.

The excess free energy of mixing is given by

$$\Delta G_{\text{mix}}^{\text{excess}} = X_1X_2(AX_2 + BX_1). \quad (5)$$

By appropriate differentiation of (4) we can obtain expressions for the partial molar free energies of mixing of components 1 and 2, respectively, thus

$$\Delta\mu_1 = RT1na_1 = \Delta G + (1 - X_1)\frac{\delta\Delta G}{\delta X_1} = (2B - A)X_1X_2^2 + AX_2^3 + RT1nX_1 \quad (6)$$

and

$$\Delta\mu_2 = RT1na_2 = \Delta G + (1 - X_2)\frac{\delta\Delta G}{\delta X_2} = (2A - B)X_1^2X_2 + BX_1^3 + RT1nX_2. \quad (7)$$

Let us consider an isostructural binary solid solution in which there is a miscibility gap. At the phase boundary,

$$\mu_{1\alpha} = \mu_{1\beta} \quad (8)$$

and

$$\mu_{2\alpha} = \mu_{2\beta}, \quad (9)$$

where 1 and 2 are components, and α and β are phases. If α and β are isostructural, a critical point is possible.

Therefore from (8) and (9), and (6) and (7),

$$(2A - B)(X_{1\alpha}^2 X_{2\alpha} - X_{1\beta}^2 X_{2\beta}) + B(X_{1\alpha}^3 - X_{1\beta}^3) + RT(1nX_{2\alpha} - 1nX_{2\beta}) = 0, \quad (10)$$

$$(2B - A)(X_{1\alpha} X_{2\alpha}^2 - X_{1\beta} X_{2\beta}^2) + A(X_{2\alpha}^3 - X_{2\beta}^3) + RT(1nX_{1\alpha} - 1nX_{1\beta}) = 0. \quad (11)$$

To simplify our equations let

$$p = X_{1\alpha}^2 X_{2\alpha} X_{1\beta}^2 X_{2\beta} = X_{1\alpha}^2(1 - X_{1\alpha}) - X_{1\beta}^2(1 - X_{1\beta}), \quad (12)$$

$$q = X_{1\alpha}^3 - X_{1\beta}^3, \quad (13)$$

$$r = RT(1nX_{2\alpha} - 1nX_{2\beta}) = RT[1n(1 - X_{1\alpha}) - 1n(1 - X_{1\beta})], \quad (14)$$

$$s = X_{1\alpha} X_{2\alpha}^2 - X_{1\beta} X_{2\beta}^2 = X_{1\alpha}(1 - X_{1\alpha}^2) - X_{1\beta}(1 - X_{1\beta})^2, \quad (15)$$

$$t = X_{2\alpha}^3 - X_{2\beta}^3 = (1 - X_{1\alpha})^3 - (1 - X_{1\beta})^3, \quad (16)$$

$$u = RT[1nX_{1\alpha} - 1nX_{1\beta}], \quad (17)$$

then

$$(2A - B)p + Bq + r = 0 \quad (18)$$

and

$$(2B - A)s + At + u = 0. \quad (19)$$

From (18) and (19) it may be shown that

$$B = \frac{r(t - s) - 2up}{4sp + (t - s)(p - q)}, \quad (20)$$

$$A = \frac{[(p - q)B - r]}{2p}. \quad (21)$$

Therefore for systems where a miscibility gap is present A and B may be calculated knowing the solubility of the two comonents 1 and 2, at a temperature T.

This model can also be applied to systems where there is no miscibility gap but activity–composition relations are available.

From Eqs. (6) and (7) it may be seen that

$$RT1n_{\gamma 1} = (2B - A)X_1 X_2^2 + AX_2^3 \quad (22)$$

and

$$RT1n_{\gamma 2} = (2A - B)X_1^2 X_2 + BX_1^3. \quad (23)$$

Therefore,

$$\frac{RT1n_{\gamma 1}}{(1 - X_1)^2} = (2B - A)X_1 + AX_2 \quad (24)$$

and

$$\frac{RT1n_{\gamma 2}}{(1 - X_2)^2} = (2A - B)X_2 + BX_1. \quad (25)$$

Thus a least-squares fit of either $RT1n_{\gamma 1}/(1 - X_1)^2$ or $RT1n_{\gamma 2}/(1 - X_2)^2$ against X_1 or X_2, respectively, should give a straight line with slope $2(B - A)$ or $2(A - B)$ and intercept A or B, respectively.

Equations similar to (20) and (21), and (24) and (25), may be obtained using a one-parameter regular solution model. In this case the free energy of mixing is given by

$$\Delta G_{mix} = WX_1X_2 + RT[X_1 1nX_1 + X_2 1nX_2]. \quad (26)$$

For systems with a miscibility gap

$$W = RT1n[(X_{1\alpha}X_{2\beta})/(X_{1\beta}X_{2\alpha})]/2(X_{2\beta} - X_{2\alpha}). \quad (27)$$

The next section considers the application of Eqs. (20), (21), (24), (25), (27), and (28) to isostructural binary and pseudobinary systems.

Results

The previous section described how to obtain the interaction parameters A and B (or W) from available solid solubility and activity–composition data. We must now consider how the magnitude of any deviations from Raoultian behavior will vary with the fundamental physical properties of the two end-members. In the introduction it was noted that four main factors affect the energetics of solid formation, namely, (1) size difference, (2) covalency difference, (3) valence, and (4) electron configuration. Of these, size difference is generally the most important.

Effects of size difference can be parameterized in three different ways. First, one

can simply consider the difference in ionic radii of the ions being mixed. Such a term, however, leads to difficulties since assignment of radii is always somewhat arbitrary. This is especially true when one tries to assign a cation radius in compounds having different anions, such as oxides, sulfides, selenides, etc. Small variations in the covalency of such compounds can drastically affect the "radii of ions." This has recently been illustrated by Shannon (*28*), who found radii of cations in sulfides to differ significantly from cationic radii in oxides.

As mentioned earlier, bond-length mismatch terms have been used to represent the size difference factor in solid solutions (*6, 12*). Such terms are more effective than ionic radii since they avoid the assignment of arbitrary radii to ions, and emphasize the importance of bond length rather than radius of one atom.

A more general and thermodynamically useful measure of the size difference term is given by a volume mismatch term. As with a bond-length term, volume mismatch does not rely on ionic radii and the volume of a phase includes the effects of small variations in covalency, as shown by Shannon and Vincent (*29*). Thus both bond-length and volume terms allow us to group together systems such as the rock salt oxides and chalcogenides. However, since volume is a basic thermodynamic parameter, its use is aesthetically preferable to bond-length terms, especially in complex crystals where coordination polyhedra do not have regular geometries.

In addition, in complex crystals, the species being mixed occupy only a small fraction of the total volume. If one compares solid solubility in CaO–MgO (very limited), $CaCO_3$–$MgCO_3$ (quite extensive), and $Ca_3Al_2Si_3O_{12}$–$Mg_3Al_2Si_3O_{12}$ (complete), one is drawn to the conclusion that greater bond-length mismatch can be tolerated by a structure in which the ions being mixed are embedded in a matrix which can itself change geometry slightly to absorb the strain. The volume mismatch term defined below allows one to include this effect.

We define the volume mismatch term

$$\Delta V = \frac{V_2 - V_1}{V_2} \quad \text{or} \quad \frac{V_2 - V_1}{V_1} \quad \text{or} \quad \frac{V_2 - V_1}{V_{\overline{12}}}, \tag{28}$$

with V_2 the molar volume of the larger component, V_1 the molar volume of the smaller component, and $V_{\overline{12}}$ the mean of the two. Thus A, the Margules parameter for the smaller ion, will be associated with a volume mismatch term $[(V_2 - V_1)/V_2]$, the term representing solution in the larger structure. Similarly, B will be associated with $[(V_2 - V_1)/V_1]$ and W with $[(V_2 - V_1)/V_{\overline{12}}]$. Note that ΔV is always defined to be positive.

Thermodynamic mixing parameters, corresponding volume mismatch terms, and temperature of experiment for rock salt oxide and chalcogenide systems are given in Table I. Data used in each system are as referenced.

In several cases, particularly the rock salt oxide systems, activity–composition relations have been determined by several different authors, and a good example is MnO–NiO (*18, 39, 54, 68, 69*). In such cases either the most recent and/or what we believe to be the most reliable data are used. Omitted from Table I is the system NiO–MgO, which is the only rock salt system so far shown to exhibit negative deviations from ideality (*16, 17*), which are probably associated with cation ordering (*16*).

The criteria for use of a regular or subregular solution model in our analysis are threefold. First, if symmetric behavior, within experimental limits of error, was observed, a regular solution is used. Second, if the data used were not considered accurate enough to warrant a two-parameter model, e.g., CaO–MgO (*47*), the one-pa-

TABLE I

THERMODYNAMIC INTERACTION PARAMETERS, CORRESPONDING VOLUME MISMATCH, AND TEMPERATURE OF EXPERIMENT FOR SOME BINARY SOLID SOLUTIONS

System	Structure	A (kJ)	B (kJ)	W (kJ)	$\frac{V_2 - V_1}{V_2}$	$\frac{V_2 - V_1}{V_1}$	$\frac{V_2 - V_1}{V_{\overline{12}}}$	T (K)	Ref.
CoO–FeO	Rock salt	—	—	3.214	—	—	0.0317	1473	(*30*)
CoO–MgO	Rock salt	—	—	4.799	—	—	0.0412	1100–1300	(*31*)
CoO–NiO	Rock salt	—	—	4.934	—	—	0.0577	1000–1300	(*32*)
CaO–CdO	Rock salt	—	—	0	—	—	0.0661	1273	(*33*)
FeO–MgO	Rock salt	—	—	15.945	—	—	0.0782	1373–1573	(*34*)
FeO–MnO	Rock salt	—	—	5.243	—	—	0.0911	1423	(*35*)
CoO–MnO	Rock salt	—	—	5.464	—	—	0.1280	1273	(*36*)
PbSe–PbTe	Rock salt	—	—	4.262	—	—	0.1570	830	(*37*)
MgO–MnO	Rock salt	—	—	18.277	—	—	0.1690	1473	(*38*)
MnO–NiO	Rock salt	—	—	12.328	—	—	0.1854	1200	(*39*)
CaO–SrO	Rock salt	—	—	23.762	—	—	0.2167	1073–1473	(*40*)
PbS–PbTe	Rock salt	18.347	22.518	—	0.2219	0.2852	—	773–1073	(*41*)
CaO–MnO	Rock salt	—	—	13.734	—	—	0.2295	1373	(*42*)
CaTe–MnTe	Rock salt	—	—	23.461	—	—	0.2299	1073–1273	(*43*)
CaSe–MnSe	Rock salt	—	—	22.255	—	—	0.2387	873–1273	(*43*)
CaS–MgS	Rock salt	25.909	29.374	—	0.2387	0.3135	—	973–1273	(*23*)
CaS–MnS	Rock salt	—	—	25.797	—	—	0.2572	1073–1273	(*23*)
MnSe–PbSe	Rock salt	18.447	37.945	—	0.2929	0.4143	—	1073	(*44*)
CaO–FeO	Rock salt	—	—	33.231	—	—	0.3190	1123–1318	(*45*)
CdO–NiO	Rock salt	—	—	40.673	—	—	0.3468	1323	(*24*)
CaO–CoO	Rock salt	—	—	30.899	—	—	0.3550	1373–1573	(*46*)
CaO–MgO	Rock salt	—	—	60.611	—	—	0.3947	2288–2703	(*47*)
CaO–NiO	Rock salt	—	—	46.091	—	—	0.4106	1373–1968	(*48*)
MnO–MnS	Rock salt	—	—	52.230	—	—	0.4761	1505	(*49*)
CO_2TiO_4–Mg_2TiO_4	Spinel	—	—	3.156	—	—	0.0011	1573	(*50*)
$Fe_3Al_2Si_3O_{12}$–$Mg_3Al_2Si_3O_{12}$	Garnet	—	—	0.816	—	—	0.0092	1200	(*51*)
$MgTiO_3$–$NiTiO_3$	Ilmenite	3.891	4.957	—	0.0175	0.0178	—	1673	(*16*)
$FeTiO_3$–$MgTiO_3$	Ilmenite	5.950	7.096	—	0.0264	0.0271	—	1573	(*52*)
Fe_2TiO_4–Mg_2TiO_4	Spinel	4.799	8.586	—	0.0337	0.0349	—	1573	(*52*)
Co_2SiO_4–Fe_2SiO_4	Olivine	—	—	3.675	—	—	0.0411	1453	(*53*)
$CoTiO_3$–$MnTiO_3$	Ilmenite	—	—	4.123	—	—	0.0530	1523	(*54*)
Fe_2SiO_4–Mg_2SiO_4	Olivine	—	—	6.380	—	—	0.0578	1477	(*55*)
$MnTiO_3$–$NiTiO_3$	Ilmenite	8.336	11.032	—	0.0750	0.0811	—	1523	(*54*)
$Ca_3Al_2Si_3O_{12}$–$Mg_3Al_2Si_3O_{12}$	Garnet	—	—	9.623	—	—	0.1008	1200	(*51*)
$CaCO_3$–$FeCO_3$	Calcite	13.845	21.133	—	0.2043	0.2568	—	573–1073	(*56*)
KI–RbI	Rock salt	—	—	5.929	—	—	0.1150	298	(*57*)
RbBr–RbCl	Rock salt	—	—	2.820	—	—	0.1218	298	(*58*)

TABLE I—*Continued*

System	Structure	A (kJ)	B (kJ)	W (kJ)	$\frac{V_2 - V_1}{V_2}$	$\frac{V_2 - V_1}{V_1}$	$\frac{V_2 - V_1}{V_{\overline{12}}}$	T (K)	Ref.
KCl–RbCl	Rock salt	—	—	1.750	—	—	0.1341	933	(*59*)
RbBr–RbI	Rock salt	4.533	6.129	—	0.1739	0.2105	—	273–333	(*60*)
KBr–KI	Rock salt	—	—	7.949	—	—	0.2053	478	(*61*)
NaBr–NaI	Rock salt	5.496	9.991	—	0.2126	0.2701	—	538	(*62*)
CsCl–TlCl	Cesium chloride	—	—	8.852	—	—	0.2172	373–473	(*63*)
KI–NaI	Rock salt	8.119	10.339	—	0.2312	0.3007	—	373–473	(*25*)
CsI–TlI	Cesium chloride	—	—	10.359	—	—	0.2514	623	(*64*)
KBr–NaBr	Rock salt	12.325	13.910	—	0.2561	0.3442	—	373–573	(*25*)
KCl–NaCl	Rock salt	12.781	16.493	—	0.2801	0.3890		473–673	(*25*)
LiCl–NaCl	Rock salt	—	—	9.760	—	—	0.2828	590	(*65*)
CsBr–TlBr	Cesium chloride	—	—	9.682	—	—	0.3449	473–523	(*66*)
NaI–RbI	Rock salt	14.004	15.612	—	0.3148	0.4595	—	691–733	(*67*)
$ZnMoO_4$–$ZnWO_4$	Wolframite	—	—	26.118	—	—	0.0038	898–1248	(*26*)
$MnMoO_4$–$MnWO_4$	Wolframite	—	—	23.600	—	—	0.0169	873–1273	(*27*)
$MnMoO_4$–$ZnMoO_4$	Wolframite	20.000	21.592	—	0.0440	0.0460	—	898–1298	(*27*)
$MnWO_4$–$ZnWO_4$	Wolframite	22.221	22.937	—	0.0564	0.0598	—	873–1073	(*27*)
$CaWO_4$–$SrWO_4$	Scheelite	21.023	28.800	—	0.1069	0.1196	—	873–1073	(*26*)
$CaWO_4$–$PbWO_4$	Scheelite	23.225	29.987	—	0.1302	0.1497	—	973	(*26*)
$BaWO_4$–$CaWO_4$	Scheelite	28.900	39.430	—	0.2205	0.2828	—	1173–1373	(*26*)

rameter model was applied. Finally, in cases where the Margules parameter for solution of the smaller ion in the larger structure, namely, A, was calculated to be larger than B, the regular solution model was used. It is recognized, however, that this last assumption may hide some real and interesting complexity.

Thermodynamic parameters of the rock salt systems given in Table I are shown as a function of the volume mismatch in Fig. 1. A linear correlation is obtained, with an almost zero intercept, between deviations from ideality and the volume mismatch term.

The linear fit gives

$$\lambda = 115.7[\Delta V] - 4.6(\text{kJ mole}^{-1}), \quad r^2 = 0.83, \quad (29)$$

where λ is A or B or W, and r is the correlation coefficient.

The correlations in these systems appear to be independent of whether the ions being mixed are anions or cations.

Table I gives results of some olivine, spinel (with no cation redistribution), ilmenite, garnet, and carbonate systems. In all these the ions being mixed are, as in the rock salt system, doubly charged and, with the exception of the garnets, in sixfold co-

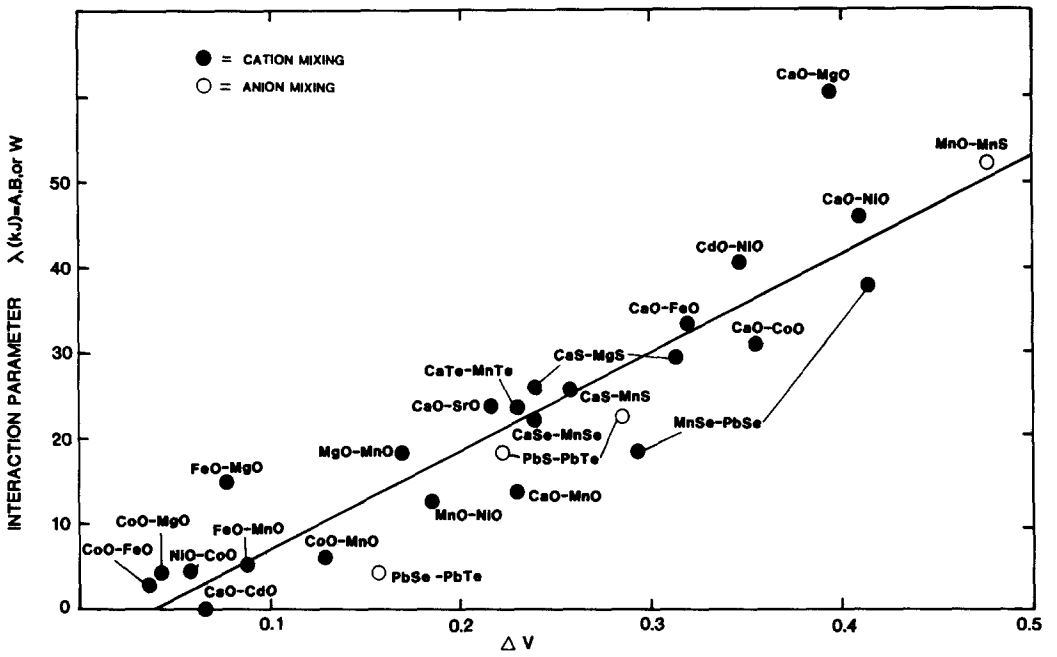

FIG. 1. Interaction parameter, λ (kJ) = *A*, *B*, or *W*, versus volume mismatch, ΔV (see text), for rock salt oxide and chalcogenide solid solutions.

ordination. Figure 2 shows a plot of these and the rock salt systems, together with a plot of the rock salt systems alone for comparison. The ternary systems appear to behave similarly to the rock salt solid solutions, the linear correlation for all systems (ternary and binary) giving

$$\lambda = 100.8[\Delta V] - 0.4(\text{kJ mole}^{-1}), \quad r^2 = 0.85. \quad (30)$$

Again, as might be expected, the correlation has an almost zero intercept. The fact that the non-rock salt systems show deviations similar to the rock salt systems suggests that structural type is not an important factor once volume differences are included in a mismatch term. That the garnet systems, in which the ion is eight-coordinated, correlate with six-coordinated systems also suggests that coordination number is not an important factor, once its effect on molar volume is taken into account.

Table I shows results on alkali halide systems. The table includes both rock salt and cesium chloride structures and some cases with cations and others anions being mixed. Results are plotted against volume mismatch in Fig. 3.

A linear correlation gives

$$\lambda = 46.9[\Delta V] - 2.7(\text{kJ mole}^{-1}), \quad r^2 = 0.79. \quad (31)$$

A major point to note is the insensitivity of the parameters to the sign of the charge of species mixed and to structure. Once more, the eight-coordinated systems (CsCl structure) appear to behave similarly to the six-coordinated ones (NaCl structure).

A much better correlation between deviations from ideality and volume mismatch may be obtained by using enthalpy of mixing data. Such enthalpy determinations, with either anions or cations being mixed, have been performed on several rock salt alkali halide systems. The enthalpy of mix-

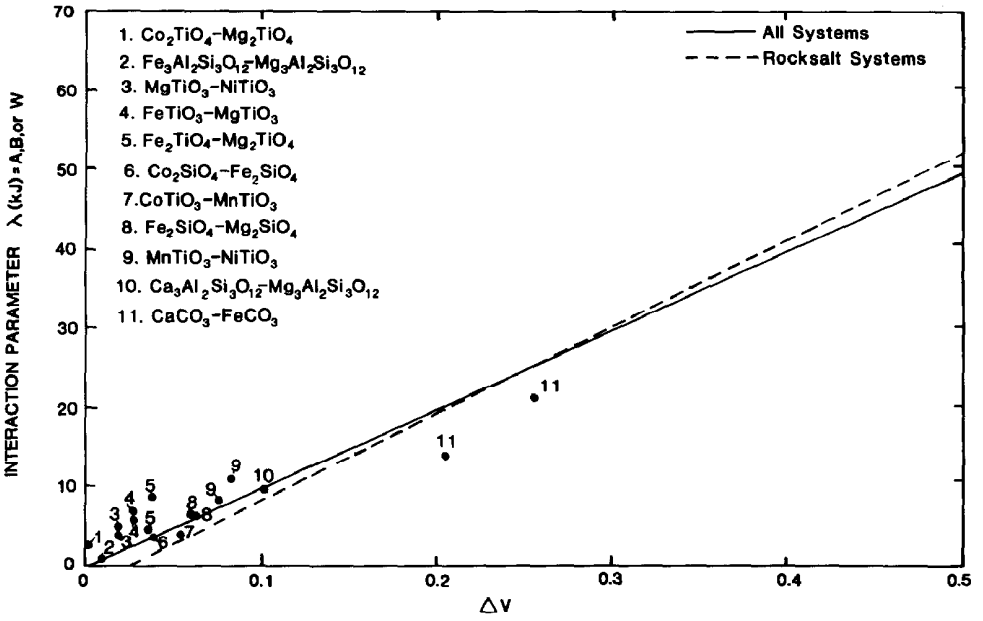

FIG. 2. Interaction parameter, λ (kJ) = *A*, *B*, or *W*, versus volume mismatch, Δ*V*, for binary solid solutions in which divalent ions are being mixed. A plot of the rock salt oxide and chalcogenide systems only is shown for comparison.

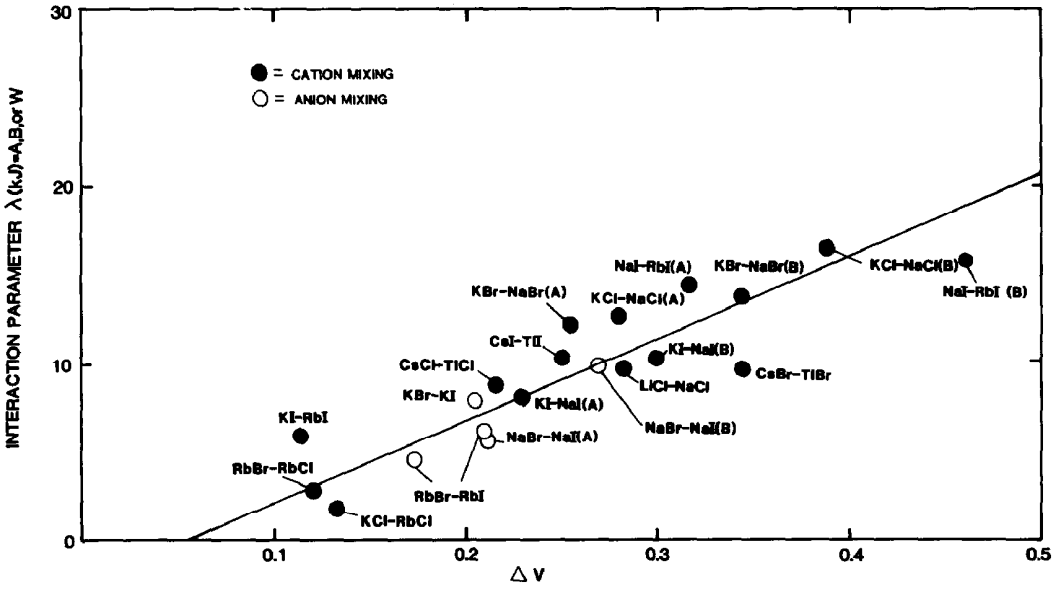

FIG. 3. Interaction parameter, λ (kJ) = *A*, *B*, or *W*, versus volume mismatch, Δ*V*, for alkali halide solid solutions.

ing parameters is given in Table II and plotted as a function of volume mismatch in Fig. 4. The mixing parameters may be fitted by a first-order correlation where

$$\lambda_H = 66.6[\Delta V] - 5.52(\text{kJ mole}^{-1}), \quad r^2 = 0.97, \quad (32)$$

with

$$\lambda_H = A_H \quad \text{or} \quad B_H \quad \text{or} \quad W_H. \quad (33)$$

As Fig. 4 shows, this correlation results in a nonzero intercept. From thermodynamic and chemical considerations, for zero volume mismatch one might expect ideal behavior in these non-transition metal systems. One can fit the data to a second-order correlation which is constrained to pass through the origin, which gives

$$\lambda_H = 124.6[\Delta V]^2 + 10.9[\Delta V] \ (\text{kJ mole}^{-1}), \quad r^2 = 0.99. \quad (34)$$

Data for some molybdate and tungstate systems are given in Table I and plotted as a function of volume mismatch in Fig. 5. A linear correlation between deviations from ideality and volume mismatch is again apparent, with

$$\lambda = 51.7[\Delta V] + 20.3(\text{kJ mole}^{-1}), \quad r^2 = 0.63. \quad (35)$$

Two points should be noted here and will be discussed later, namely, the insensitivity to whether cations or anions are being mixed, and the much higher relative deviations, with a large nonzero intercept, exhibited by these molybdates and tungstates compared to the other systems.

Discussion

The results obtained show that one can find linear or quadratic relations between thermodynamic mixing parameters and a term representing the difference in molar volume between the two end-members.

This approach gives good correlations for all systems on which data in the literature are available. The use of volume mismatch

TABLE II

ENTHALPY INTERACTION PARAMETERS AND CORRESPONDING VOLUME MISMATCH TERMS FOR SOME ROCK SALT ALKALI HALIDE AND ROCK SALT OXIDE BINARY SOLID SOLUTIONS

System	A_H (kJ)	B_H (kJ)	W_H	$\frac{V_2 - V_1}{V_1}$	$\frac{V_2 - V_1}{V_2}$	$\frac{V_2 - V_1}{V_{\overline{12}}}$	Ref.
KI–RbI	2.410	2.950	—	0.1088	0.1220	—	(57)
KCl–RbCL	3.371	4.084	—	0.1257	0.1437	—	(70)
KBr–KCl	—	—	4.030	—	—	0.1411	(71)
NaBa–NaCl	5.227	6.001	—	0.1598	0.1902	—	(70)
KBr–KI	—	—	7.437	—	—	0.2053	(72)
KBr–NaBr	12.274	16.944	—	0.2561	0.3442	—	(72)
KI–NaI	—	—	10.614	—	—	0.2614	(72)
NaBr–NaI	7.981	11.846	—	0.2126	0.2704	—	(72)
KCl–NaCl	—	—	18.485	—	—	0.3256	(72)
MgO–NiO	—	—	−14.622	—	—	0.0165	(73)
CoO–MgO	—	—	0	—	—	0.0412	(73)
CoO–NiO	—	—	0	—	—	0.0577	(73)
CaO–CdO	—	—	—	—	—	0.0661	(73)
FeO–MgO	—	—	5.021	—	—	0.0782	(34)
CoO–MnO	—	—	6.010	—	—	0.1280	(18)
MgO–MnO	—	—	17.085	—	—	0.1690	(74)
MnO–NiO	—	—	9.987	—	—	0.1854	(18)

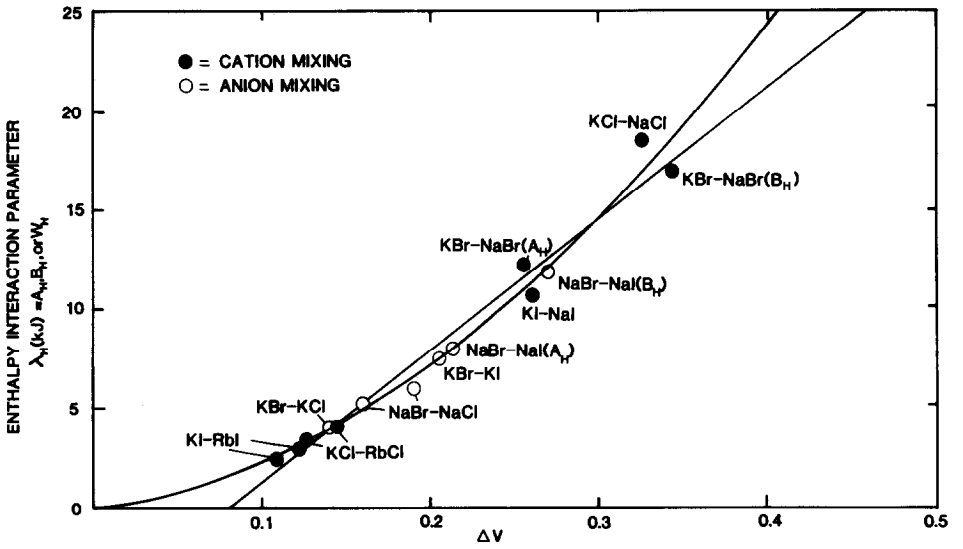

FIG. 4. Enthalpy interaction parameter, λ_H (kJ) = A_H, B_H, or W_H, versus volume mismatch, ΔV, for rock salt alkali halide solid solutions.

instead of ionic radii mismatch as a measure of deviations from ideality has allowed us to group together many more systems than would otherwise be possible. Thus oxide, sulfide, selenide, and telluride systems with rock salt structure can all be correlated by Eq. (29) when related to the volume mismatch term. Furthermore, essentially the same correlation can be extended with equal accuracy to all systems in which the

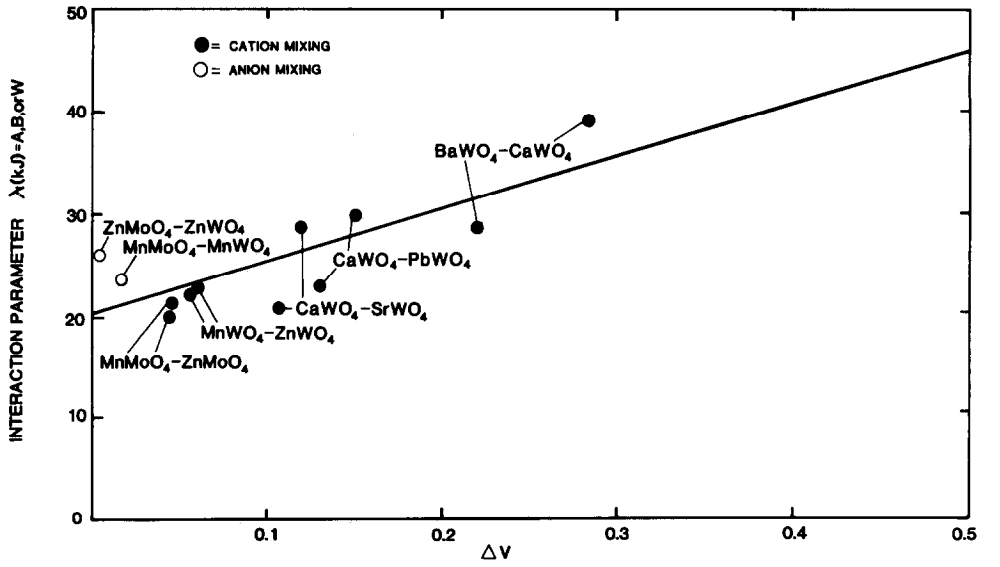

FIG. 5. Interaction parameter, λ (kJ) = A, B, or W, versus volume mismatch, ΔV, for tungstate and molybdate solid solutions.

ions being mixed are doubly charged, except for molybdates and tungstates. This suggests that the correlation is rather insensitive to details of structural type and coordination number.

Silicate systems are of geochemical interest. Silicates generally have larger molar volumes and correspondingly smaller volume mismatch terms than corresponding rock salt systems. One can confidently predict, therefore, that pseudobinary silicate systems (with no cation or anion redistributions) should show fairly small positive excess free energies of mixing, quantitative estimates being obtained from Eq. (30).

The correlations also suggest that both anion mixing and cation mixing result in similar relations between energy parameters and volume mismatch terms. Although data on anion mixing are generally rather limited for systems other than alkali halides, the few data for oxide and chalcogenide systems and the more abundant alkali halide data are sufficient to demonstrate this point.

Figure 6 shows all the correlations for alkali halides, rock salt oxides and chalcogenides, and tungstates and molybdates. It is apparent that the volume mismatch term segregates these systems into three distinct groups. The alkali halide systems as a group show much smaller position deviations from ideality than the rock salt oxide and chalcogenide systems. This is a result of the different valence of the ions being mixed. The slopes of the correlations represent the difference between mixing singly charged ions in the halides and doubly charged ions in the oxides and chalcogenides. From Eqs. (29) and (31) the ratio of the slopes is calculated to be 2.5. One might expect the difference in slope to be related by the term (z_+z_-), which, if all the compounds were truly ionic, would give a ratio of slopes of 4. The smaller difference in observed slopes therefore reflects deviations from completely ionic behavior.

Hazen and Finger (*75*) estimated relative ionicities of bonds, denoted S^2, in alkali halides, oxides, and chalcogenides. S^2, assumed to be constant for a given anion, was defined as 0.5 for the oxides and calculated

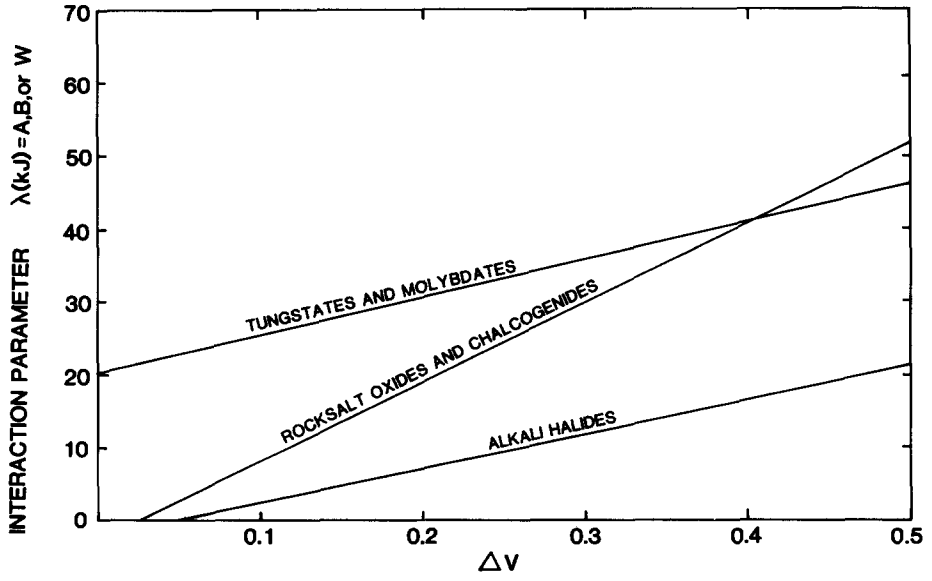

FIG. 6. Linear correlations of interaction parameters and volume mismatch for alkali halide, rock salt oxide and chalcogenide, and tungstate and molybdate systems.

to be 0.4 for chalcogenides and 0.75 for alkali halides. Using a weighted average of 0.47 for S^2 in the oxide and chalcogenide systems the ratio of the product $S^2(Z^+Z^-)$ in these and the alkali halides is 2.5. That this corresponds exactly to the observed ratio of the slopes of the correlations may be fortuitous; however, it strongly suggests that the difference in slope is a result of the difference in effective charge of the oxides and chalcogenides, and the alkali halides.

Deviations in the molybdate and tungstate systems are somewhat surprising. Again a linear correlation is observed with no dependence upon which type of ion is being mixed. These compounds crystallize at atmospheric pressure with either a wolframite or a scheelite structure, the type of structure adopted depending upon the ionic radius of the cation (*76*). In scheelite the divalent cation is eight-coordinated and in tungsten four-coordinated, and in wolframite all cations are six-coordinated. This study finds similar deviations from ideality for both scheelite and wolframite systems. This is consistent with findings for the singly and doubly charged systems in which structure and coordination number appear to have little effect upon the observed correlations. However, in Fig. 6 one sees that the tungstates and molybdates as a group exhibit much larger deviations from ideality than other systems, and that these deviations are similar whether the anion group or divalent cations are being mixed. Both findings are hard to explain. The covalent nature of the XO_4^{2-} group is well recognized and this covalency is thought to lead to a strongly ionic M–O bond. If these differences between the XO_4^{2-} group and the M–O bond are related to the energetics of mixing, it is surprising that the energetics are unaffected by whether anions or cations are being mixed.

So far the results have been discussed in terms of size, charge, and covalency. In the case of transition metal-containing systems, we must also consider effects of electron configuration.

Alkali halide systems, in which all ions have filled shell configurations, would not be expected to show any electron configuration effects. Thus, as shown in Fig. 4, a second-order correlation, constrained to pass through the origin, was used to fit the alkali halide enthalpy data. In systems containing transition metals, however, electron configuration effects are possible. Table II shows regular solution enthalpy parameters for some rock salt oxide solid solutions. Although deviations from ideality appear to increase as the volume mismatch increases, the rate of increase is somewhat irregular, and negative deviations occur in the NiO–MgO system.

Electron configurational effects are necessarily specific to the particular transition metal ion and any resultant energetic stabilization can, at present, only be accurately determined by direct experimental measurement. Systems found to show negative deviations are the $CoTiO_3$–$MgTiO_3$ ilmenite series (*50*), Co_2TiO_4–Mn_2TiO_4 and Ni_2TiO_4–Mn_2TiO_4 spinel systems (*54*), the Ni_2SiO_4–Mg_2SiO_4 olivine system (*17*), and NiO–MgO rock salt solid solutions (*16, 17*). Deviations in the olivine system are presumably due to an ordering of the cations on the octahedral $M1$ and $M2$ sites, while deviations in the spinel systems may also be a result of some cation redistribution. However, negative deviations in the $CoTiO_3$–$MgTiO_3$ and NiO–MgO solid solutions appear to be a result of electron configuration effects alone. Such effects in the NiO–MgO system have been discussed elsewhere (*16*).

Applications

Prediction of Solid Solubility

Probably the most obvious application of the correlations is to the prediction of ex-

pected solubilities and activity–composition relations as a function of temperature. Many systems, for example, sulfides, selenides, and tellurides, are experimentally difficult to work with, in part because of nonstoichiometry. Knowing only the molar volume of the end-members, one can predict expected deviations from ideality from these correlations.

Considered here are binary systems in which the ions being mixed are doubly charged. Subregular mixing parameters can be predicted from Eq. (30).

By manipulation of equations given under Thermodynamic Formalisms it is possible to calculate the solvus and critical mixing temperature and composition from the parameters A and B. At the critical temperature, the third and second derivatives of the total free energy, with respect to both components, are equal to zero.

Therefore it can be shown that, at the critical point,

$$RT_{(c)} = 2X_{1(c)}(2A - B) + 2X_{1(c)}^2(4B - 5A) + 6X_{1(c)}^3(A - B) \quad (36)$$

with

$$X_{1(c)} = 1 - X_{2(c)} = \frac{4(5A - 4B) \pm \sqrt{16(4B - 5A)^2 - 144(2A - B)(A - B)}}{36(A - B)}. \quad (37)$$

$X_{1(c)}$ and $X_{2(c)}$ may therefore be calculated from A and B from Eq. (37) and substitution into Eq. (36) yields $T_{(c)}$. Predictions of A, B, $T_{(c)}$, $X_{1(c)}$, and $X_{2(c)}$ for binary systems, in which doubly charged ions are being mixed, with volume differences ranging from 5 to 45% are given in Table III.

The solvi for these systems can also be calculated by calculating activities of both components, at various temperatures, from Eqs. (6) and (7). At the phase boundary $a_{1\alpha} = a_{1\beta}$ and $a_{2\beta} = a_{2\alpha}$. The resulting solvi are shown in Fig. 7.

This treatment can be applied to real systems whose solubilities are extremely limited and thus are experimentally difficult to determine. Good examples are BaO–MgO, BeO–ZnO, and CaO–CaS. Predicted solubilities up to 2200K are given in Table IV.

Prediction of Deviations from Ideality in High-Pressure Silicate Solid Solutions

Using Eq. (30) it is possible to predict deviations from ideality in high-pressure phases of geological significance.

Under lower-mantle conditions ilmenite and perovskite may become important silicate phases. Although $FeSiO_3$ is not known

TABLE III

PREDICTED CRITICAL TEMPERATURES AND COMPOSITIONS OF MIXING FOR VARIOUS COMPONENT SIZE DIFFERENCES

Component size difference (%)	$\frac{V_2 - V_1}{V_2}$	$\frac{V_2 - V_1}{V_1}$	A (kJ)	B (kJ)	T_c (K)	$X_{1(c)}$	$X_{2(c)}$
5	0.0488	0.0513	4.745	5.992	293	0.52	0.48
15	0.1395	0.1622	13.715	15.951	903	0.55	0.45
25	0.2222	0.2857	21.887	28.162	1555	0.59	0.41
35	0.2979	0.4242	29.364	41.854	2274	0.61	0.39
45	0.3673	0.5806	36.230	57.311	3089	0.63	0.37

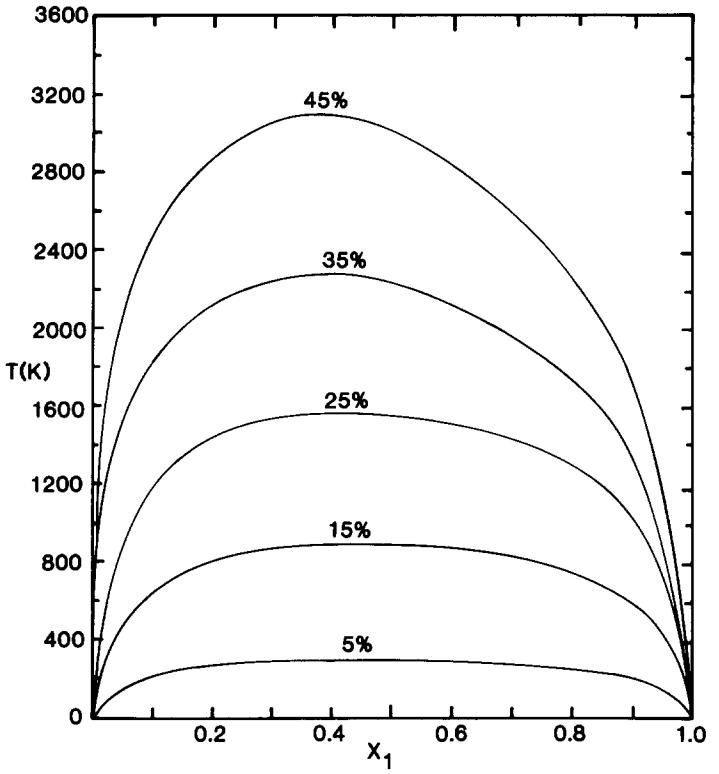

FIG. 7. Predicted solvi for binary systems for various component size differences. The percentage size difference in each case is shown.

TABLE IV

PREDICTED SOLUBILITY LIMITS IN SOME BINARY SYSTEMS

System	A (kJ)	B (kJ)	T (K)	$X_{2\alpha}$	$X_{1\beta}$
BeO–ZnO	41.484	71.684	1600	<0.005	0.05
			1800	0.005	0.07
			2000	0.0125	0.0975
			2100	0.015	0.105
			2200	0.025	0.125
BaO–MgO	55.666	127.786	1700	<0.005	0.1075
			1800	<0.005	0.0026
			2000	<0.005	0.0325
			2100	<0.005	0.0375
CaO–CaS	39.616	66.242	1000	<0.005	0.0075
			1400	<0.005	0.035
			1600	0.007	0.055
			1800	0.015	0.085
			2000	0.025	0.115
			2200	0.035	0.145

as a pure ilmenite or perovskite, its molar volume can be predicted using solid solubility data (*77*) and crystal chemical correlations (*78*). Thus the molar volume of $FeSiO_3$, ilmenite, may be estimated from X-ray measurements on the $MgSiO_3$–$FeSiO_3$ ilmenite solid solution series (*77*). Using the crystal chemical correlations of Yagi *et al.* (*78*) and Shannon's ionic radii (*79*), the molar volume of $FeSiO_3$, perovskite, is calculated for both high-spin and low-spin Fe^{2+}.

End-member molar volumes and calculated interaction parameters, for 1 mole of ions being mixed, for the Mg–Fe spinel, ilmenite, and perovskite silicate solid solutions, are given in Table V. For all solid solutions, moderate positive deviations are predicted, except for low-spin Fe^{2+}

TABLE V

CALCULATED THERMODYNAMIC PROPERTIES OF Mg–Se MIXING IN HIGH-PRESSURE SILICATES

Structure	V_{Mg}^{molar} (cm³)	V_{Fe}^{molar} (cm³)	A^a (kJ)	B^a (kJ)
Spinel	39.58	42.04	5.86	5.87
Ilmenite	26.76	23.97[b]	7.63	8.32
Perovskite	25.22[c]	24.09[d]	4.08	4.29
		25.82[e]	1.96	2.03

[a] Per ion being mixed.
[b] Estimated from solid solubility—Ref. (*77*).
[c] Calculated from Ref. (*78*).
[d] Calculated from Ref. (*78*)—low-spin Fe^{2+}.
[e] Calculated from Ref. (*78*)—high-spin Fe^{2+}.

perovskites, which, under high-pressure conditions, may be the most stable, where very small positive deviations would be expected.

Prediction of the Energetics of Phase Transitions

This application concerns nonisostructural systems, which usually show only limited solubility. Knowing the terminal solid solubilities and expected deviations from ideality in the two regions of solid solubility, one can calculate the free energy of the phase transition each end-member must undergo to be soluble in the other. Terminal solubilities have been experimentally determined in a number of systems and deviations from ideality may be estimated from the present correlations.

Direct experimental measurement of the energetics of phase transitions in the alkaline earth and transition metal oxides and chalcogenides is not often possible. Most occur uniquely as one phase at accessible pressure and temperature conditions. Others, e.g., BaO, SrO, and CaO, undergo high-pressure transitions to nonquenchable phases. A few, e.g., MnSe and MnTe, are polymorphic at atmospheric pressure. Thus one must resort to solid solution formation to estimate such transition energies to hypothetical structures or krypto modifications.

Presented are calculations for the rock salt to nickel arsenide transition, and rock salt (or nickel arsenide) to wurtzite (or sphalerite) transition, in some oxides and chalcogenides.

Thermodynamic formalism. As before, components are 1 and 2 and phases are α and β. However, α and β now are not isostructural. Component 1, on dissolving in the component 2-rich β phase, must necessarily undergo a phase transition from α to β. The chemical potential of 1 in phase β will be composed of three terms: (1) the standard chemical potential, μ_1^0, in its stable structure, α, (2) the change in chemical potential, $\Delta\mu$, due to the phase change $\alpha \rightarrow \beta$, and (3) the change in the chemical potential, $RT\ln a_{1\beta}$, due to the solid solution of 1, with structure β, with 2, where $a_{1\beta}$ is the activity of 1 in 2 relative to β as a standard state.

Therefore,

$$\mu_{1\beta} = \mu_1^0 + \Delta\mu_{1_{\alpha\rightarrow\beta}} + RT\ln a_{1\beta}. \quad (38)$$

The chemical potential of component 1 in its own phase α is given by

$$\mu_{1\alpha} = \mu_1^0 + RT\ln a_{1\alpha}. \quad (39)$$

Since, at the phase boundary, $\mu_{1\alpha} = \mu_{1\beta}$, we have

$$RT\ln a_{1\alpha} = \Delta\mu_{1_{\alpha\rightarrow\beta}} + RT\ln_{1\beta}. \quad (40)$$

Therefore

$$\Delta\mu_{1_{\alpha\rightarrow\beta}} = RT\ln(a_{1\alpha}/a_{1\beta}) \quad (41)$$

and similarly

$$\Delta\mu_{1_{\beta\rightarrow\alpha}} = RT\ln(a_{2\beta}/a_{2\alpha}). \quad (42)$$

We can calculate $a_{1\alpha}$, $a_{1\beta}$, $a_{2\alpha}$, and $a_{2\beta}$ at the limits of solubility from the correlations given previously and the molar volumes of 1 and 2 in phases α and β.

Usually the molar volumes of component 1 in structure β and component 2 in structure α (that is, the molar volumes of the

krypto modifications) have not been experimentally determined. A reliable means of estimating molar volumes of these phases is achieved by use of correlations of molar volume and the function $(r_{cation} + r_{anion})^3$. For the phases investigated, namely, rock salt, nickel arsenide, and wurtzite (or sphalerite), such volume plots are shown in Fig. 8, the radii used being those of Shannon (*79*). In each case an excellent linear correlation is obtained; for rock salt phases,

$$V^0 = 1.077\,(r_{anion} + r_{cation})^3 + 1.75\ \text{cm}^3\ \text{mole}^{-1}, \quad R^2 = 0.98; \quad (43)$$

for nickel arsenide,

$$V^0 = 1.121\,(r_{anion} + r_{cation})^3 - 0.39\ \text{cm}^3\ \text{mole}^{-1}, \quad R^2 = 0.91; \quad (44)$$

and for wurtzite/sphalerite phases,

$$V^0 = 1.457\,(r_{anion} + r_{cation})^3 + 2.693\ \text{cm}^3\ \text{mole}^{-1}, \quad R^2 = 0.99; \quad (45)$$

That nonzero intercepts result from these plots may well reflect the deviation of these structures from ideal close packing. Note that these correlations use the cube of the sum of ionic radii, that is, the cube of the bond length, which is a term having dimensions of volume and insensitive to the choice of individual radii. Molar volumes obtained from Eqs. (43), (44), and (45) were used to estimate A and B using Eq. (30).

TABLE VI

CALCULATED FREE ENERGIES FOR ROCK SALT TO NICKEL ARSENIDE TRANSITIONS

Compound	ΔG (kJ mole^{-1})	Ref.
MnTe	0	(*80*)
MnSe	3.068	(*80, 81*)
FeSe	−5.619	(*82*)
CoSe	−3.280	(*83*)
NiSe	−5.607	(*83*)
MgS	57.582	(*23*)
MnS	11.988	(*23*)
FeS	−2.427	(*23, 84*)

Rock salt to nickel arsenide transformation. The nickel arsenide structure occurs in the transition metal chalcogenides while

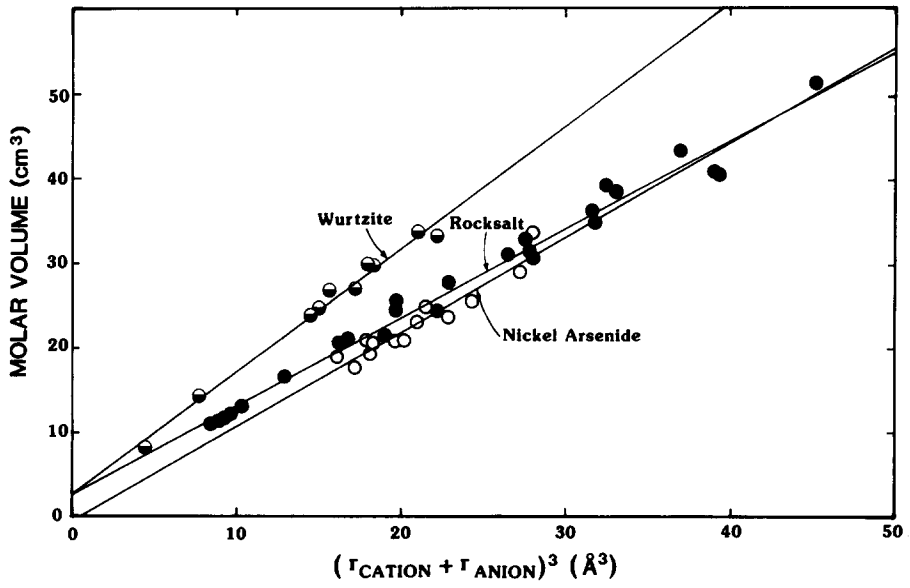

FIG. 8. Molar volume (cm³/mole) versus the cube of the sum of ionic radii for wurtzite and sphalerite, rock salt, and nickel arsenide structures.

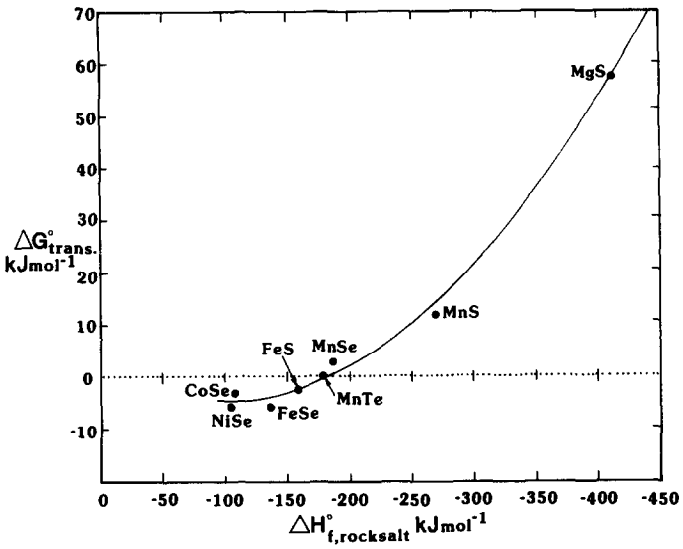

FIG. 9. Standard free energies, ΔG°_{trans}, of the rock salt to nickel arsenide transformation as a function of the standard enthalpy of formation, ΔH°_{f}, of the rock salt phase at 298K.

the rock salt structure occurs in the alkaline earth oxides and chalcogenides and transition metal oxides. Using the above technique the free energy of the transition for rock salt to nickel arsenide structures was calculated for several chalcogenide systems (see Table VI). All molar volume data used to calculate the subregular solution parameters were taken from the correlations given by Eqs. (43) and (44).

TABLE VII

CALCULATED FREE ENERGIES FOR WURTZITE/SPHALERITE (FOURFOLD COORDINATION) TO ROCK SALT/NICKEL ARSENIDE (SIXFOLD COORDINATION) TRANSITIONS

Compound	ΔG (kJ mole^{-1})	Ref.
CdTe	16.573	(*86*)
ZnTe	51.442	(*86*)
CdSe	8.367	(*86, 87*)
MnSe	−4.712	(*87, 88*)
ZnSe	31.326	(*86, 88*)
CdS	5.603	(*86, 89*)
CoS	−8.703	(*90*)
FeS	−5.623	(*91*)
MnS	−4.451	(*89, 92, 93*)
NiS	−33.063	(*94*)
ZnS	56.647	(*86*)
CdO	−14.856	(*95*)
CoO	−15.164	(*3*)
MgO	−35.861	(*96*)
MnO	−13.622	(*96*)
NiO	−28.535	(*3*)
ZnO	24.267	(*3*)

Also shown are free energy data for MnSe and MnTe, where the transition is experimentally observable, ΔG being calculated from the observed transition pressure and molar volume change.

Using the data given in Table VI, it was recently shown (*85*) that estimates can be made of free energies of transformation from rock salt to nickel arsenide structure in oxides from a plot of the free energy of transition against the standard enthalpy of formation of the rock salt phase (see Fig. 9). It is observed that as the enthalpy of formation of the rock salt phase becomes less negative, i.e., the phase becomes less ionic, the more metallic and covalent NiAs structure becomes more competitive.

Transitions from fourfold to sixfold coordination. Wurtzite and sphalerite structures, in which cations and anions are in

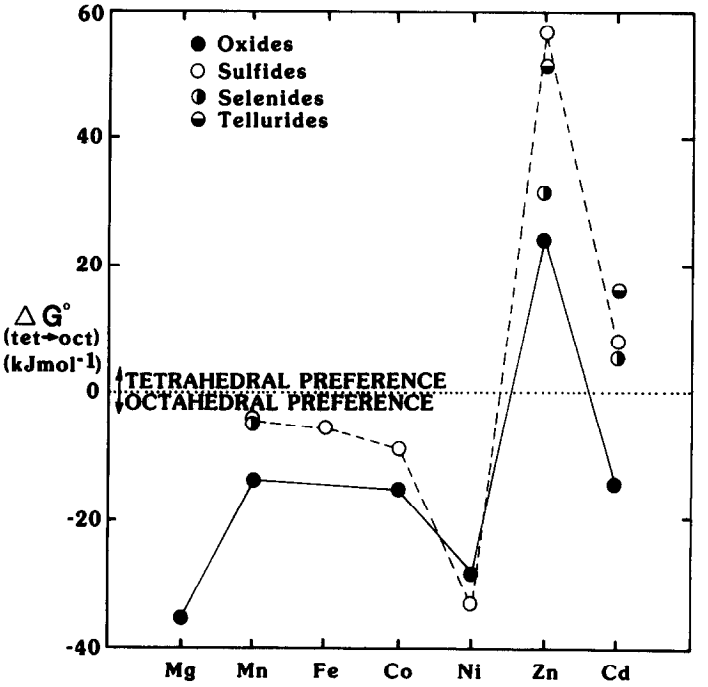

FIG. 10. Octahedral and tetrahedral preference energies, $\Delta G^{\circ}_{tet \rightarrow oct}$, of cations in some binary oxides and chalcogenides.

tetrahedral coordination, commonly occur in oxides and chalcogenides. Transitions from these to octahedral coordination in rock salt or nickel arsenide structures involve a large negative volume change (see Fig. 8). Values for the free energy of these transitions can be calculated from available solid solubility data using the treatment described previously. In several compounds, transitions are experimentally observable, free energies in these cases are calculated from the observed transition pressure and molar volume differences. Data thus calculated for some oxides and chalcogenides are given in Table VII.

As would be expected, crystal field stabilizations play a major role in determining the energy of transformation for the transition metal-containing compounds. Figure 10 shows that, in accordance with crystal field effects and covalency, preference for octahedral coordination increases in the order Zn < Cd < Mn, Fe Co < Ni, Mg. The preference for tetrahedral coordination is slightly greater for chalcogenides than for oxides, but the overall patterns of stability remain the same.

Acknowledgment

This work was supported by the National Science Foundation (Grants 78-10038 and 81-06027).

References

1. J. A. WASASTJERNA, *Soc. Sci. Fenn. Commentat. Phys. Math.* **14,** 5 (1948).
2. R. W. TAYLOR, *Amer. Mineral.* **49,** 1016 (1964).
3. A. NAVROTSKY AND A. MUAN, *J. Inorg. Nucl. Chem.* **33,** 35 (1971).
4. D. L. FANCHER AND G. R. BARSCH, *J. Phys. Chem. Solids* **30,** 2503 (1969).
5. V. S. URUSOV, *Geokhimiya* **4,** 510 (1970).
6. A. NAVROTSKY, "M.T.P. Int. Rev. Sci., Inorg. Chem." (D. W. A. Sharp, Ed.), Series 2, Vol. 5, p. 29 (1974).
7. O. J. KLEPPA AND S. . MESCHEL, *J. Phys. Chem.* **69,** 3531 (1965).

8. F. C. M. Driessens, *Ber. Bunsenges. Phys. Chem.* **82,** 754 (1968).
9. D. L. Fancher and G. R. Barsch, *J. Phys. Chem. Solids* **30,** 2517 (1969).
10. D. L. Fancher and G. R. Barsch, *J. Phys. Chem. Solids* **32,** 1303 (1971).
11. B. G. Dick and T. P. Das, *Phys. Rev.* **127,** 1053 (1962).
12. V. S. Urusov, *Geokhimiya* **9,** 1033 (1968).
13. Y. P. Ostapchenko, *Izv. Akad. Nauk SSSR Ser. Fiz.* **20,** 10 (1956).
14. N. A. Toropov and I. F. Fedorov, *Zh. Neorg. Khim.* **9,** 8 (1964).
15. F. C. M. Driessens, *Ber. Bunsenes. Phys. Chem.* **72,** 764 (1968).
16. P. K. Davies and A. Navrotsky, *J. Solid State Chem.* **38,** 264 (1981).
17. Y. Shirane, *Kuamoto Diagaku Kogakubu Kenkyu Hokoku* **28**(3), 133 (1979).
18. C. R. Catlow, B. E. Fender, and P. J. Hampson, *J. Chem. Soc. Faraday Trans. II* **73,** 911 (1977).
19. J. D. Dunitz and L. E. Orgel, *Phys. Chem. Solids.* **3,** 311 (1957).
20. O. J. Kleppa, *Annu. Rev. Phys. Chem.* **16,** 187 (1965).
21. M. Blander, *J. Chem. Phys.* **34,** 697 (1961).
22. A. Navrotsky, *Phys. Chem. Miner.* **2,** 89 (1977).
23. B. J. Skinner and F. D. Luce, *Amer. Mineral.* **56,** 1269 (1971).
24. N. V. Komilova and L. A. Bashkirov, *Izv. Akad. Nauk SSSR Neorg. Mat.* **13**(10), 851 (1977).
25. N. B. Chanh, *J. Chim. Phys.* **61,** 1428 (1964).
26. L. L. Y. Chang, *Amer. Mineral.* **52,** 427 (1967).
27. L. L. Y. Chang, *Miner. Mag.* **36**(283), 992 (1968).
28. R. D. Shannon, "Structure and Bonding in Crystals" (M. O'Keefe and A. Navrotsky, Eds.), Vol. II, p 53. Academic Press, New York (1982).
29. R. D. Shannon and H. Vincent, *Struct. Bonding (Berlin)* **19,** 1 (1974).
30. E. Aukrust and A. Muan, *Trans. AIME* **227,** 1378 (1963).
31. M. Rigaud, G. Giovanetti, and M. Hone, *J. Chem. Thermodyn.* **6,** 993 (1974).
32. K. Torkar and R. Schneider, *J. Solid State Chem.* **18,** 89 (1976).
33. K. K. Prasad, Ph.D. thesis, *Ind. Inst. Sci.*, Banglore (1972).
34. W. C. Hahn, Jr., and A. Muan, *Trans. AIME* **224,** 416 (1962).
35. F. Schwerdtfeger and A. Muan, *Trans. AIME* **239,** 1114 (1967).
36. S. Seetharaman and K. P. Abraham, *Scr. Metall.* **3,** 911 (1969).
37. Shamsuddin and S. Misra, *Z. Metallkd. Bd.* **70,** 541 (1979).
38. W. C. Hahn, Jr., and A. Muan, *Mater. Res. Bull.* **5,** 955 (1970).
39. H. Paulsson and E. Rosen, *Chem. Scr.* **11,** 2 (1977).
40. A. Bergstein, *Czech. J. Phys. B* **23,** 1141 (1973).
41. V. N. Romanenko and A. F. Sidorov, *Izv. Akad. Nauk SSSR Neorg. Mat.* **11,** 3, 432 (1975).
42. N. Tiberg and A. Muan, *Metall. Trans.* **1,** 435 (1970).
43. Chi-Hung Leung and L. Van Vlack, *J. Amer. Ceram. Soc.* **62,** 11/12, 613 (1970).
44. V. G. Vanyarkho, V. P. Zlomanov, A. V. Novoselova, and V. N. Fokin, *Izv. Akad. Nauk SSSR Neorg. Mat.* **5**(10), 1699 (1969).
45. F. Abbatista, A. Burdese, and M. Maja, *Rev. Int. Hautes Temp. Refract.* **12,** 337 (1975).
46. A. Muan, *J. Inorg. Nucl. Chem.* **32,** 5, 1457 (1970).
47. R. C. Doman, J. B. Barr, R. N. McNally, and A. M. Alper, *J. Amer. Ceram. Soc.* **46,** 63, 313 (1964).
48. D. E. Smith, T. Y. Tien, and L. H. Van Vlack, *J. Amer. Ceram. Soc.* **52,** 8, 459 (1969).
49. H. C. Chao, Y. E. Smith, and L. H. Van Vlack, *Trans. AIME* **227,** 796 (1963).
50. B. Brezny and A. Muan, *Thermochim. Acta* **2,** 107 (1971).
51. H. O'Neill and B. Wood, *Contrib. Mineral. Petrol.* **70,** 59 (1979).
52. R. E. Johnson, E. Woermann, and A. Muan, *Amer. J. Sci.* **271,** 278 (1971).
53. D. P. Masse, E. Rosen, and A. Muan, *J. Amer. Ceram. Soc.* **49,** 328 (1966).
54. L. G. Evans and A. Muan, *Thermochim. Acta* **2,** 277 (1971).
55. K. Kitayama and T. Katsura, *Bull. Chem. Soc. Japan* **41,** 1146 (1968).
56. J. R. Goldsmith, D. L. Graf, J. Witters, and D. A. Northrup, *J. Geol.* **70,** 6, 659 (1962).
57. G. R. Allakhverdov, N. I. Sorokin, and B. D. Stepin, *Zh. Fiz. Khim.* **49,** 3013 (1975).
58. L. L. Makarov, Y. G. Vlasov, and V. I. Izotov, *Russ. J. Phys. Chem.* **38,** 10, 1297 (1964).
59. R. Lindström, *Ann. Acad. Sci. Fenn. Ser. A6* **398,** 1 (1972).
60. M. Ahtee and H. Koski, *Ann. Acad. Sci. Fenn. Ser. A6* **297,** 1 (1968).
61. P. Luova and O. Tannila, *Suom. Kemistil. B* **39,** 220 (1966).
62. N. B. Chanh, Thése de doctorat, Université de Bordeaux (1965).
63. A. Schiraldi, E. Pezzati, and G. Chiodelli, *Z. Phys. Chem. Neue Folge Bd.* **113,** 189 (1978).
64. A. Schiraldi, E. Pezzati, and P. Rossi, *Z. Phys. Chem. Neue Folge Bd.* **121,** 17 (1980).

65. A. SMITS, J. ELGERSMA, AND H. V. HARDENBERG, *Res. Trav. Chim.* **43,** 671 (1924).
66. A. SCHIRALDI, E. PEZZATI, AND G. CHIODELLI, *Z. Phys. Chem. Neue Folge Bd.* **110,** 1 (1978).
67. R. G. SAMUSOVA AND V. E. PLYUSHCHEV, *Russ. J. Inorg. Chem.* **9**(10), 1315 (1964).
68. W. C. HAHN, JR., AND A. MUAN, *J. Phys. Chem. Solids* **19,** 3/4, 338 (1961).
69. D. J. CAMERON AND A. E. UNGER, *Metall. Trans.* **1,** 2615 (1970).
70. V. HOVI, *Acta Metall.* **2,** 334 (1956).
71. N. Fontell, V. Hovi, and A. Mikkola, *Ann. Acad. Sci. Fenn. Ser. A1* **54** (1948).
72. M. W. LISTER AND N. F. MEYERS, *J. Phys. Chem.* **62,** 145 (1958).
73. P. K. DAVIES, Ph.D. thesis, Arizona State University (1981).
74. H. GRIPENBERG, S. SEETHARAMAN, AND L. L. STAFFANSSON, *Chem. Scr.* **13,** 162 (1979).
75. R. M. HAZEN AND L. W. FINGER, *J. Geophys. Res.* **84**(B12), 6723 (1979).
76. A. W. SLEIGHT, *Acta Crystallogr. Sect. B* **28,** 2899 (1972).
77. L. G. LIU, *Phys. Earth Planet. Inter.* **11,** 289 (1976).
78. T. YAGI, H. K. MAO, AND P. M. BELL, *Phys. Chem. Miner.* **3,** 97 (1978).
79. R. D. SHANNON, *Acta Crystallogr. Sect. A* **32,** 751 (1976).
80. W. D. JOHNSTON AND D. E. SESTRICH, *J. Inorg. Nucl. Chem.* **19,** 229 (1961).
81. L. CEMIC AND A. NEUHAUS, *High Temp. High Pressures* **4,** 97 (1972).
82. G. S. MANN AND L. VAN VLACK, *Metall. Trans. B* **8,** 47 (1977).
83. V. N. KAMAT DALAL, H. V. KEER, AND A. B. BISWAS, *J. Inorg. Nucl. Chem.* **33,** 2839 (1971).
84. M. FISCHER AND K. SCHWERDTFEGER, *Metall. Trans. B* **8,** 457 (1972).
85. A. NAVROTSKY AND P. K. DAVIES, *J. Geophys. Res.* **86,** B5, 3689 (1981).
86. C. J. M. ROOYMANS, Ph.D. thesis, University of Amsterdam (1967).
87. H. WIEDEMEIER AND A. G. SIGAI, *J. Solid State Chem.* **2,** 404 (1970).
88. L. CEMIC AND A. NEUHAUS, *High Temp. High Pressures* **6,** 203 (1974).
89. H. D. LUTZ AND W. BECKER, *J. Solid State Chem.* **20,** 183 (1977).
90. W. BECKER AND H. D. LUTZ, *Mater. Res. Bull.* **13,** 907 (1978).
91. M. FLEET, *Amer. Mineral.* **60,** 466 (1975).
92. F. A. KROGER, *Z. Kristallogr. A* **100,** 543 (1938).
93. F. A. KROGER, *Z. Kristallogr. A* **102,** 132 (1939).
94. G. K. CZAMANSKI AND F. E. GOFF, *Econ. Geol.* **68,** 258 (1973).
95. J. J. BROWN AND F. A. HUMMEL, *J. Electrochem. Soc.* **111**(9), 1052 (1964).
96. A. NAVROTSKY AND D. S. KENNY, *J. Inorg. Nucl. Chem.* **34,** 2115 (1972).